

Effect of dendron structures on the luminescent and charge transporting properties of solution processed OLEDs

Mile Gao,¹ Van T. N. Mai,¹ Junhyuk Jang,¹ Chandana Sampath Kumara Ranasinghe,¹ Ronan Chu,¹ Paul L. Burn,^{1*} Ian R. Gentle,¹ Almantas Pivrikas,² Paul E. Shaw¹

¹Centre for Organic Photonics & Electronics, The School of Chemistry and Molecular Biosciences, The University of Queensland, Queensland, Australia, 4072.

²Physics Department, Murdoch University, Perth, Western Australia 6150.

*Email: p.burn2@uq.edu.au

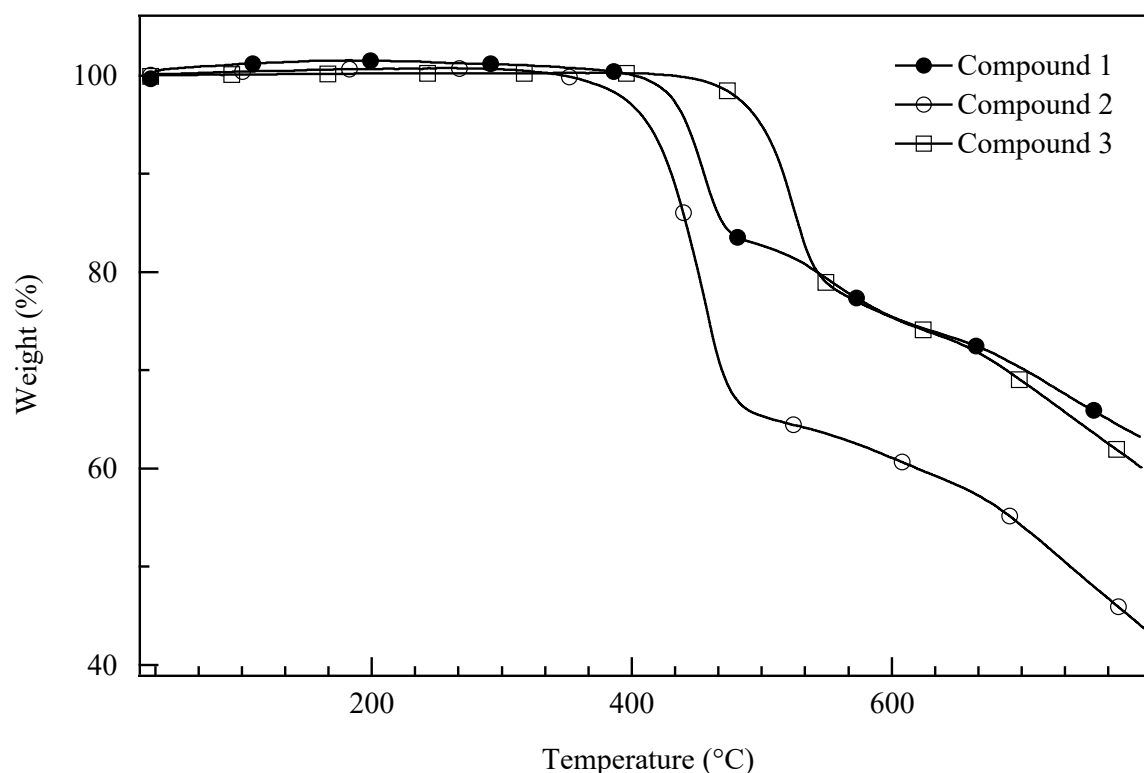


Fig. S1 Thermogravimetric analysis (TGA) trace of the hosts **1**, **2**, and **3** with a heating rate of $10\text{ }^{\circ}\text{C min}^{-1}$ under nitrogen.

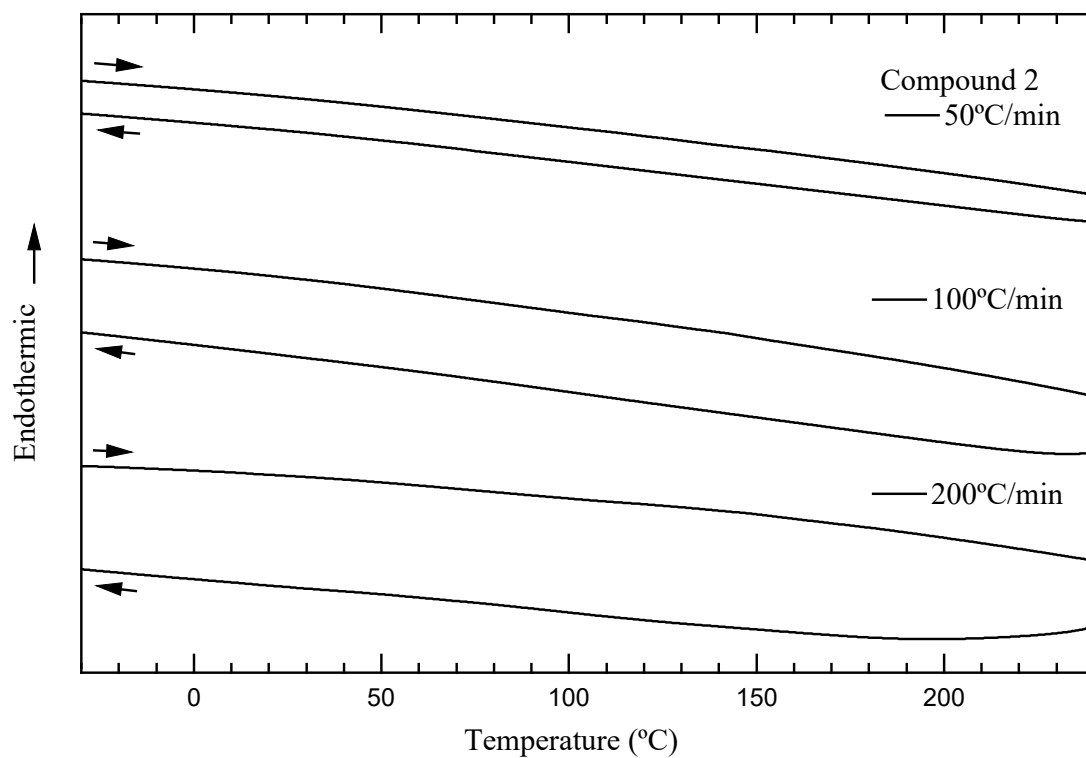


Fig. S2 Heat flow traces (for the 2nd heating cycle) of **2** scanned from -30 °C to 240 °C with scan rates of 50 °C min⁻¹ and 100 °C min⁻¹.

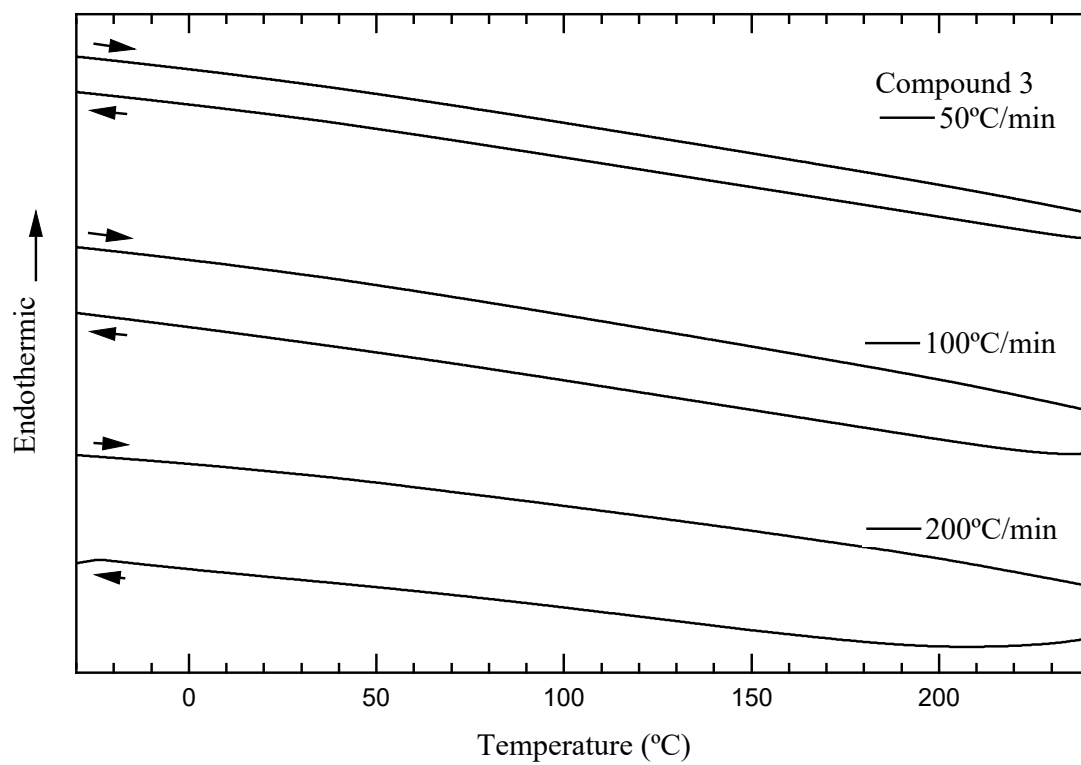


Fig. S3 Heat flow traces (for the 2nd heating cycle) of **3** scanned from -30 °C to 240 °C with scan rates of 50 °C min⁻¹, 100 °C min⁻¹, and 200 °C min⁻¹.

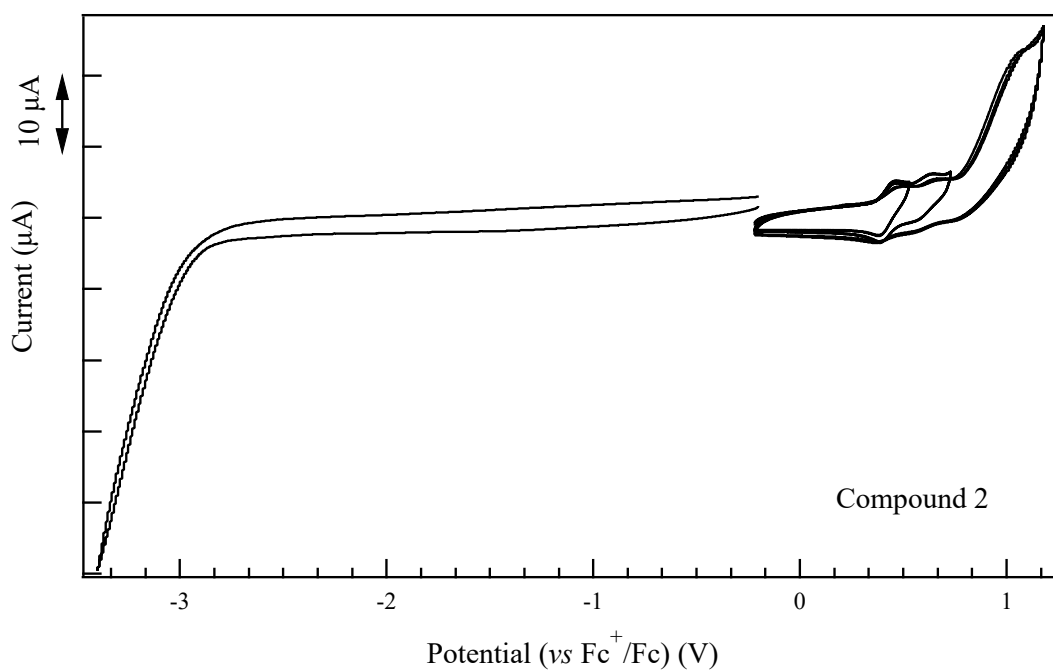


Fig. S4 Cyclic voltammograms of **2** referenced to the ferrocene/ferrocenium couple measured in tetrahydrofuran (for reduction) and dichloromethane (for oxidation) at a 1 mM concentration. Measurements were conducted with a 0.1 M tetra-*n*-butylammonium perchlorate as the electrolyte; working electrode = glassy carbon; reference electrode = 0.01 M AgNO₃ in acetonitrile; counter electrode = platinum; scan rate = 100 mV s⁻¹ (for reduction) and 50 mV s⁻¹ (for oxidation).

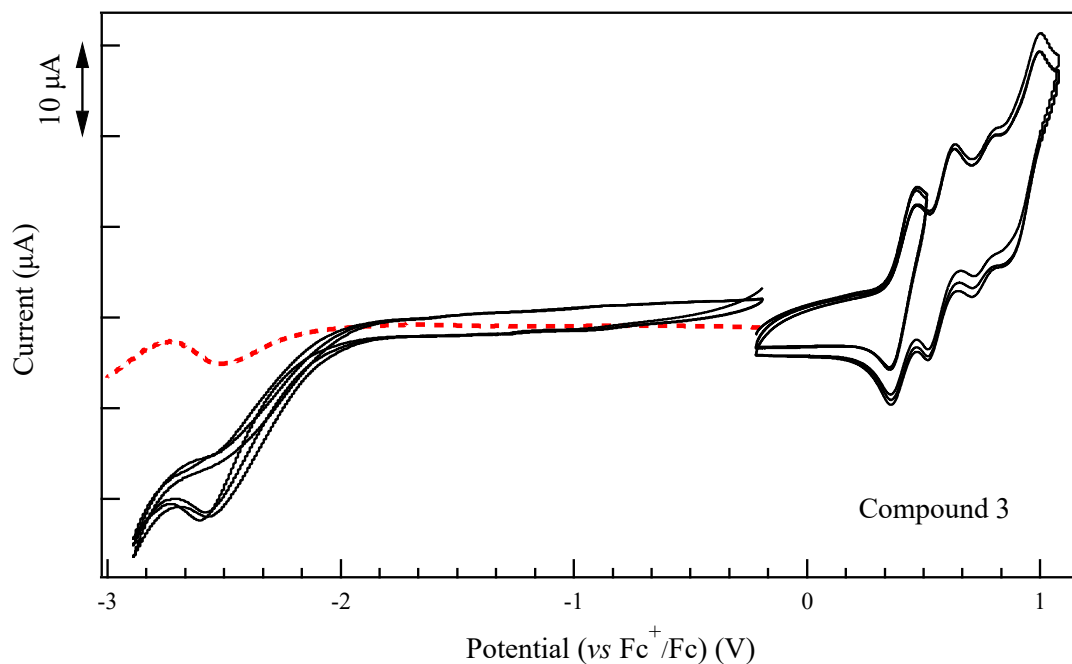


Fig. S5 Cyclic voltammograms of **3** referenced to the ferrocene/ferrocenium couple measured in tetrahydrofuran (for reduction) and dichloromethane (for oxidation) at a 1 mM concentration. Measurements were conducted with a 0.1 M tetra-*n*-butylammonium perchlorate as the electrolyte; working electrode = glassy carbon; reference electrode = 0.01 M AgNO₃ in acetonitrile; counter electrode = platinum; scan rate = 50 mV s⁻¹ (for reduction) and 100 mV s⁻¹ (for oxidation).

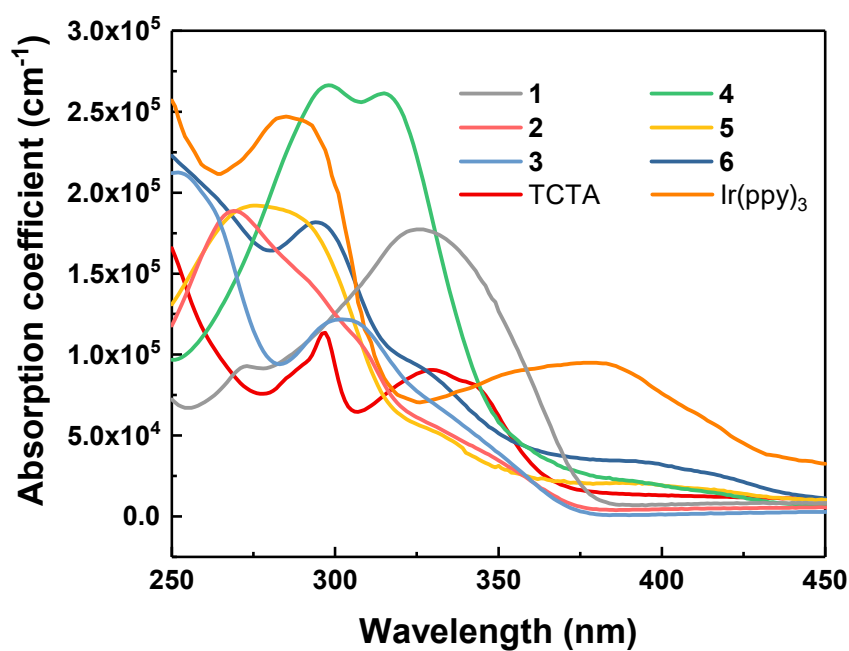
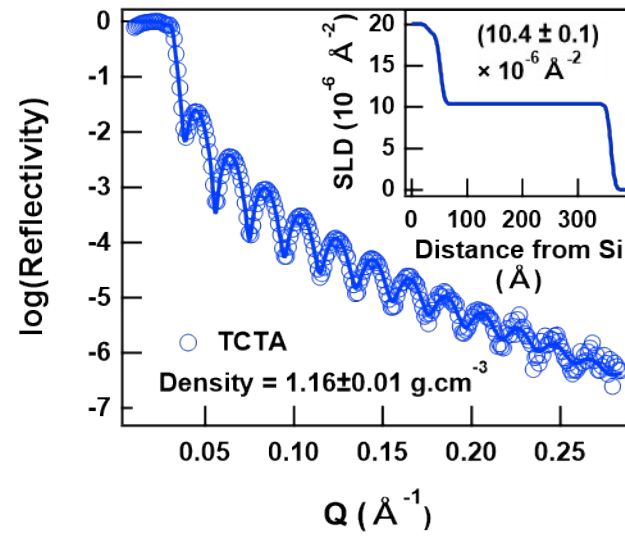
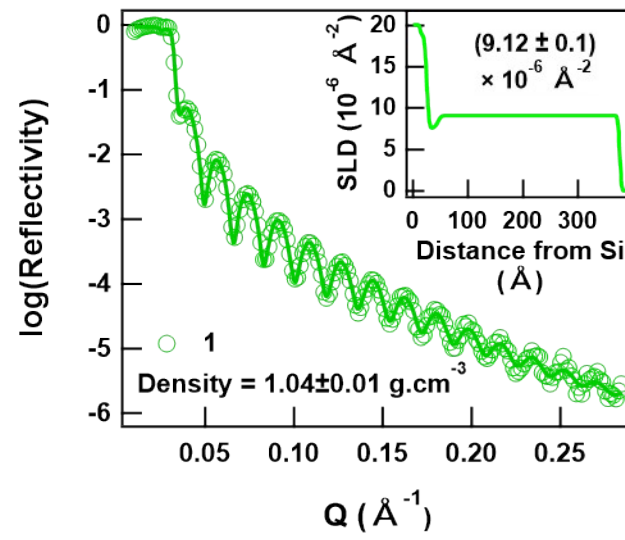


Fig. S6 Absorption coefficients of the materials.

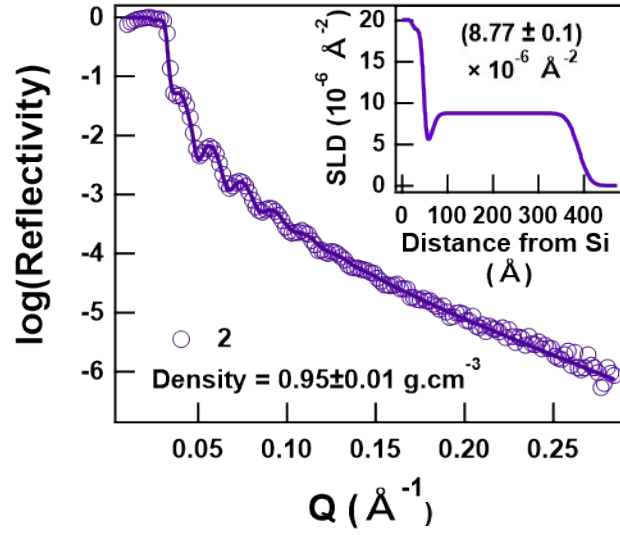
(a)



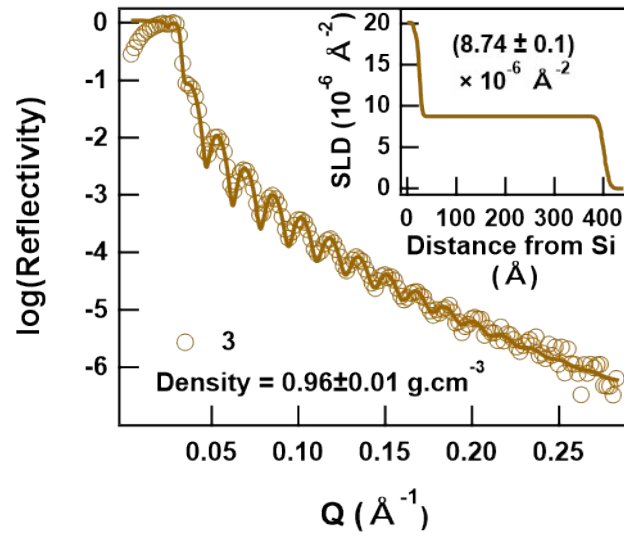
(b)



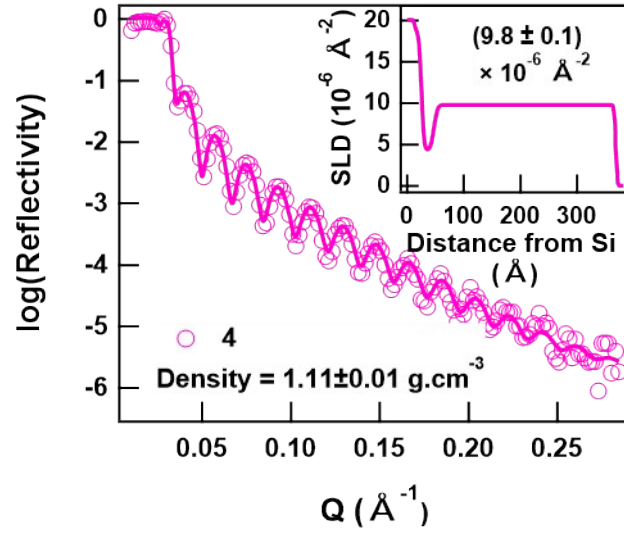
(c)



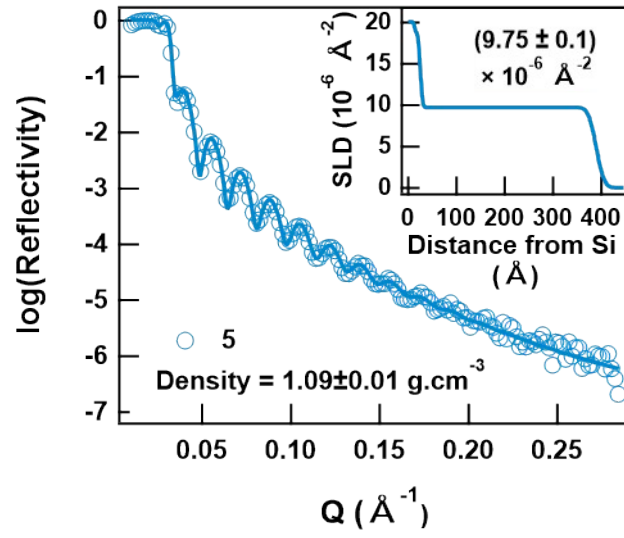
(d)



(e)



(f)



(g)

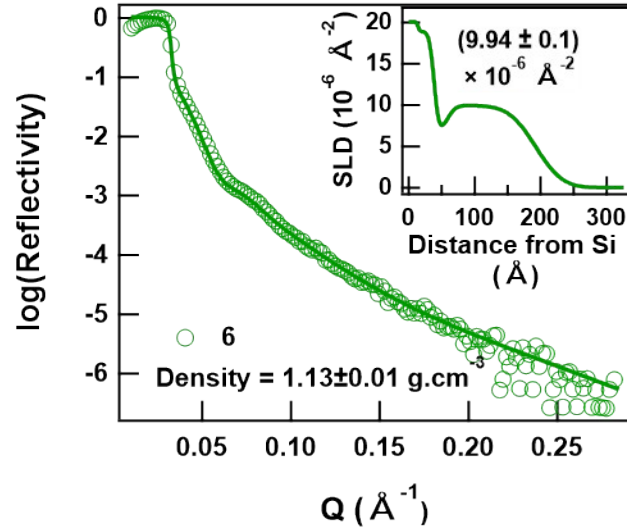
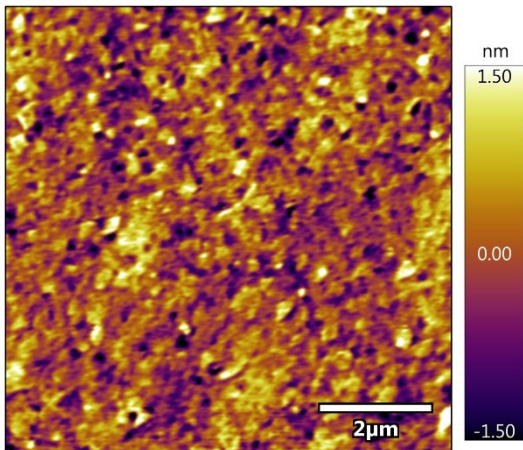
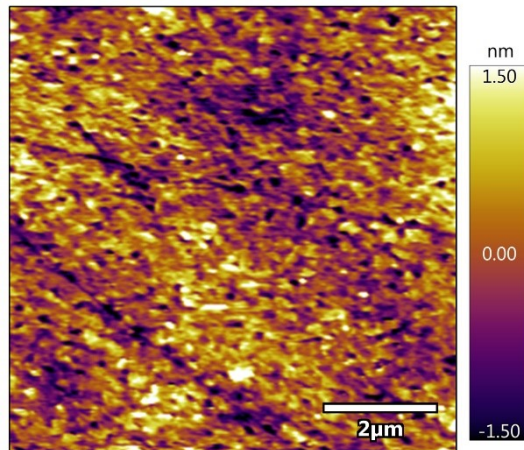


Fig. S7 X-ray reflectometry (XRR) profiles and corresponding scattering length density (SLD) versus thickness plots (insets) for (a) TCTA, (b) 1, (c) 2, (d) 3, (e) 4, (f) 5, (g) 6. Individual points represent experimental data and solid lines indicate the fitting curves.

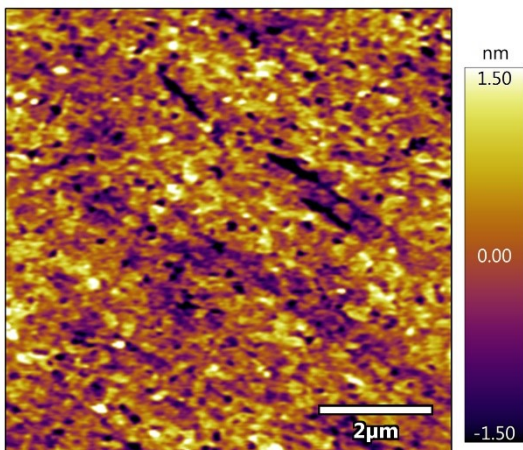
Neat 1



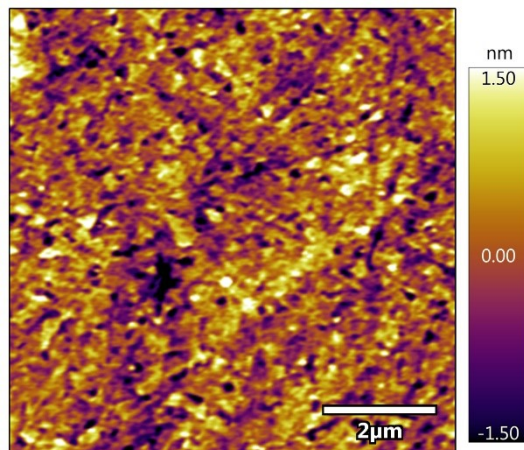
Neat 4



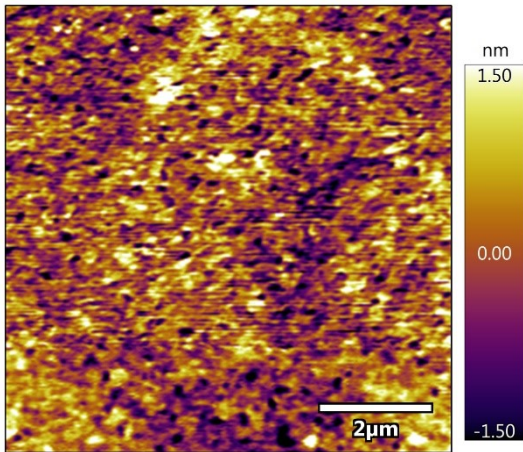
11 mol% 1 & 4 blend



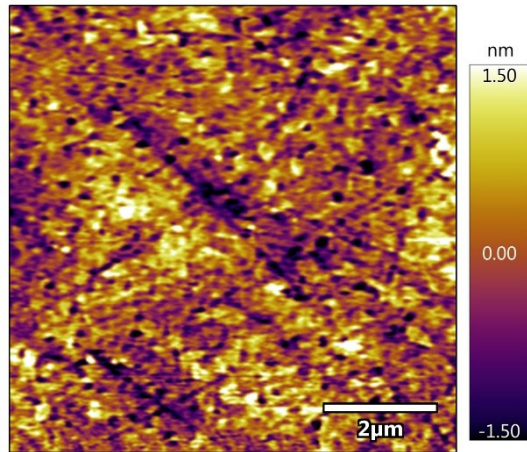
22 mol% 1 & 4 blend



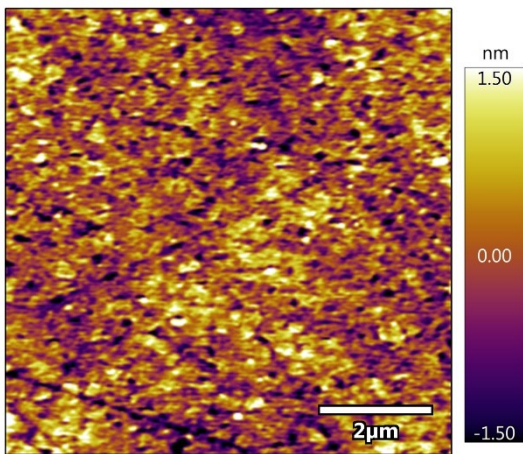
Neat 2



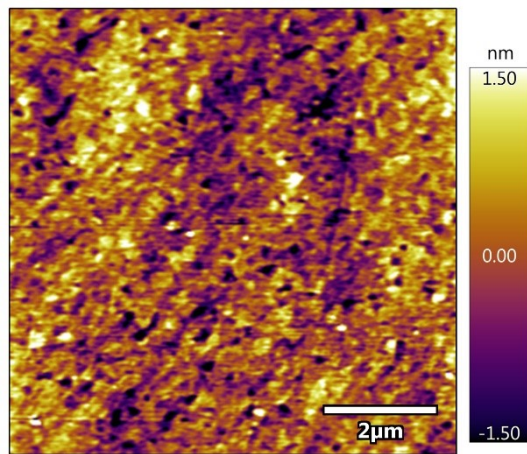
Neat 5



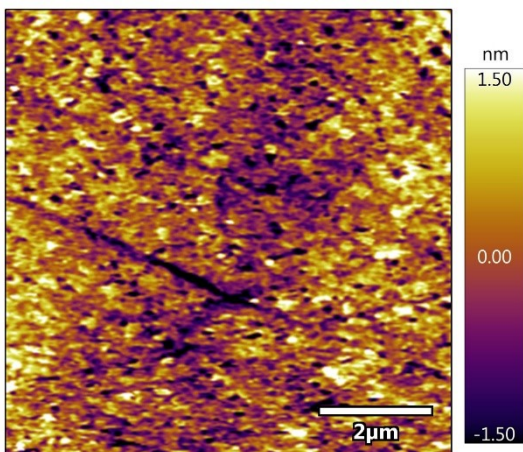
11 mol% 2 & 5 blend



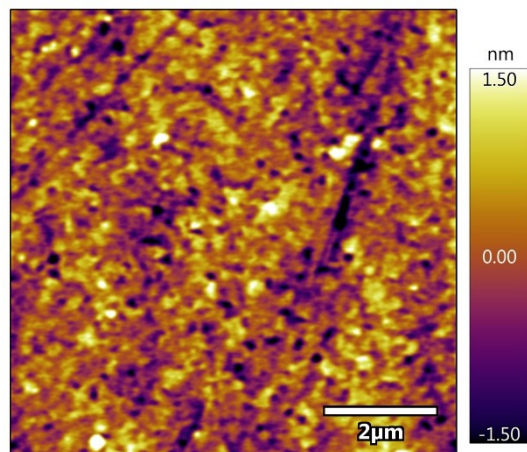
22 mol% 2 & 5 blend



Neat 3



Neat 6



11 mol% 3 & 6 blend

22 mol% 3 & 6 blend

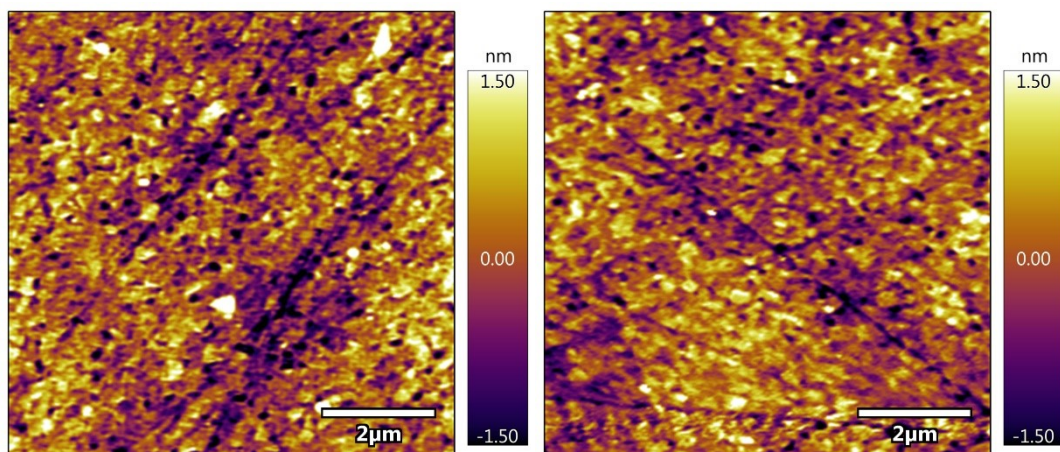


Fig. S8 AFM images of the neat and blend films.

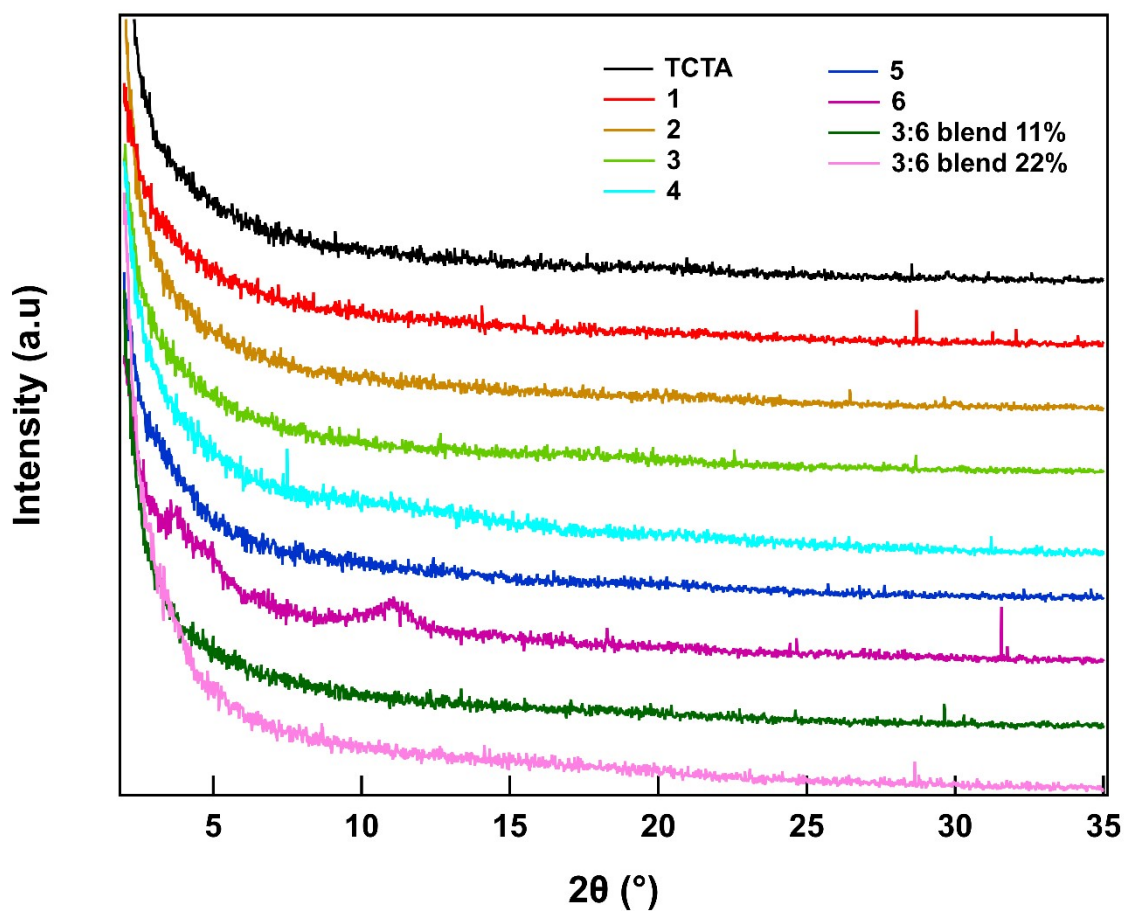


Fig. S9 Grazing incidence X-ray diffraction spectra of compounds. Data has been offset for clarity and the 3:6 blends are in mol%.